

Passivity-Based Control of an Overhead Travelling Crane

Harald Aschemann*

* Chair of Mechatronics, University of Rostock, 18059 Rostock,
Germany (e-mail: harald.aschemann@uni-rostock.de)

Abstract: In this paper, a passivity-based control scheme is proposed for the two main translational axes of an overhead crane to provide an active damping of crane load oscillations. The decentralised control structure consists of independent axis controllers, which are adapted to the varying rope length using gain-scheduling techniques. The tracking capabilities concerning desired trajectories for the crane load in the xy -plane can be improved by introducing feedforward control based on an inverse system model. Furthermore, a reduced-order disturbance observer is utilised for the compensation of nonlinear friction forces. The achieved control performance is shown by selected experimental results obtained from an implementation on a 5 t-overhead travelling crane. *Copyright ©2008 IFAC*

Keywords: Mechatronics, crane control, passivity, tracking, nonlinear systems

1. INTRODUCTION

In the last decade, numerous model-based trajectory control schemes for overhead travelling cranes have been proposed by different authors. Besides non-linear control approaches exploiting differential flatness (Boustany et al. [1992]), gain-scheduling techniques have proved efficient (Aschemann et al. [2000], Nguyen [1994]). Aiming at an increased handling frequency and a fully automated crane operation, the focus has to be on the movement of the crane load. Trajectory control concepts for automated bridge cranes allow for following specified trajectories in the workspace with small tracking errors and time optimal trajectory planning becomes important. In practical implementations, however, tracking accuracy as well as steady-state accuracy strongly depend on the inclusion of appropriate control action to counteract nonlinear disturbances, especially nonlinear friction acting on the drives as the dominant disturbance. Furthermore, a robust or adaptive control approach is necessary as regards varying system parameters like rope length or load mass during crane operation (Nguyen [1994]).

The considered 5 t-overhead crane consists of six actuated axes, where the x -, y - and z -axes as the translational main axes allow for positioning of the crane load in the three-dimensional workspace as shown in fig. 1. The crane load can be hoisted or lowered in z -direction by means of the rope suspension. The x -axis represents the direction of the bridge motion, whereas the direction of the trolley motion on the bridge is referred to as y -axis. In order to operate a high rack storage, the crane has been upgraded with an orientation unit that is equipped with three additional axes, each actuated by an torque controlled DC-motor. Feedforward and feedback control as well as observer based disturbance compensation are adapted to varying system parameters by gain-scheduling. The developed controller allows for trajectory control concerning the crane load position as well as active oscillation damping concerning

all six load degrees of freedom (Aschemann [2002]). By this, the capabilities of an automated overhead crane are extended considerably and, moreover, it can be considered as a robot manipulator that combines the capability of handling heavy loads with a large workspace.

In this paper, the first principle modelling of the two main translational crane axes is addressed first. Aiming at a decentralised control structure, for each axis a separate design model is derived in symbolic form. At this, the derived state space model is reformulated as Port-Hamiltonian-System as starting point for the envisaged passivity-based control following the energy-shifting method and the IDA-PBC approach, respectively (Lozano et al. [2000], Rodriguez et al. [2000], van der Schaft [2000], Janzen [2006]). The control design for the y -axis involves the control of the corresponding crane load position in y -direction, whereas the multi-variable control of the x -axis deals with both the crane load position in x -direction and the position difference of the two bridge drives, corresponding to a skew of the crane bridge. Feedforward control based on an inverse system model and friction compensation using disturbance observer have proved efficient to further reduce tracking errors. Thereby, desired trajectories for the crane load position in the xz -plane can be tracked independently with high accuracy. Experimental results of the closed-loop system show both excellent tracking performance and steady-state accuracy.

2. NONLINEAR MODELLING

As a decentralised control structure is envisaged, a separate design model of is used for each crane axis. Here, the modelling shall be presented only for the y -axis. The origin of the y -axis, $y_k = 0$, is located in the middle of the bridge. With a bridge length $l_{br} = 8.7\text{ m}$ the available workspace in y -direction is characterised by $y_k \in [-4.35\text{ m}, 4.35\text{ m}]$. The crane axis is modelled as a multibody system with two rigid bodies as shown in fig. 2. The trolley is modelled

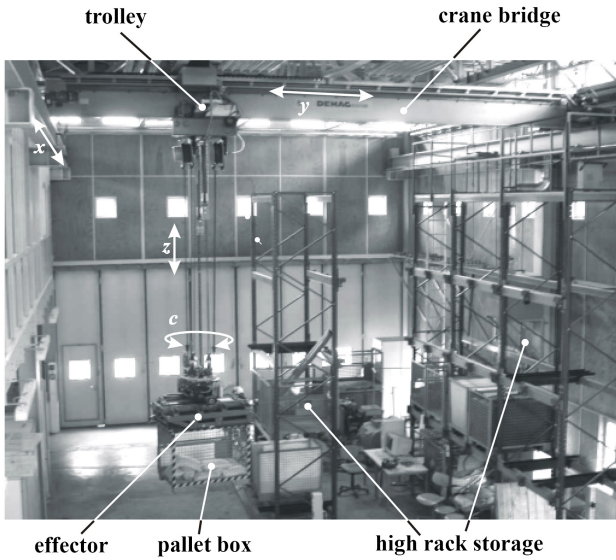


Fig. 1. Structure of the overhead travelling crane

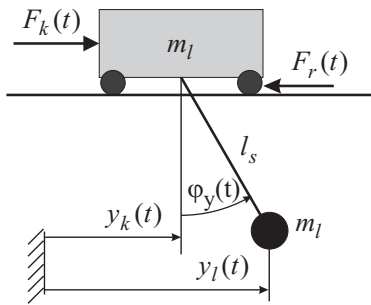


Fig. 2. Mechanical model of the y -axis

by a mass m_k , whereas the crane load is represented by a lumped mass m_l . The trolley is electrically driven by a motor force F_k . As the main disturbance nonlinear friction and damping are taken into account by the disturbance force F_r . This disturbance force is neglected at feedback control design but counteracted by both feedforward and observer-based disturbance compensation. The rope suspension is considered as massless connection, where rope deflections and small external damping are neglected. The equations of motion are derived by using Lagrange's equations. The number of the degrees of freedom for the mechanical model of the y -axis is given by $f = 2$. Consequently, a complete and unique kinematic description involves two generalised coordinates, which are chosen here as trolley position y_k and as the crane load position y_l .

The state variables for the y -axis are chosen as the generalised coordinates as well as their time derivatives, i.e. the according velocities. The rope length l_s is considered as slowly varying parameter and, hence, not introduced as state variable. The state vector \underline{x} is given by

$$\underline{x} = [y_k, y_l, \dot{y}_k, \dot{y}_l]^T. \quad (1)$$

For the derivation of the equation of motions Lagrange's equation shall be employed. The Lagrangian represents the difference between the kinetic energy T and the potential energy V

$$T = \frac{1}{2} m_k \dot{y}_k^2 + \frac{1}{2} m_l \dot{y}_l^2,$$

$$V = -m_l g l_s \cos(\varphi_y) = -m_l g l_s \cos\left(\arcsin\left(\frac{y_l - y_k}{l_s}\right)\right)$$

$$= -m_l g l_s \sqrt{1 - \frac{(y_l - y_k)^2}{l_s^2}}. \quad (2)$$

Then, the Lagrangian can be calculated as $\mathcal{L} = T - V$. The evaluation of Lagrange's equations results in the equations of motion for the crane y -axis

$$m_k \ddot{y}_k - \frac{m_l g (y_l - y_k)}{l_s \sqrt{1 - \frac{(y_l - y_k)^2}{l_s^2}}} = F_k - F_r, \quad (3)$$

$$m_l \ddot{y}_l + \frac{m_l g (y_l - y_k)}{l_s \sqrt{1 - \frac{(y_l - y_k)^2}{l_s^2}}} = 0. \quad (4)$$

With neglected friction, i.e. $F_r = 0$, the corresponding state space representation becomes

$$\dot{\underline{x}} = \begin{bmatrix} \dot{y}_k \\ \dot{y}_l \\ \ddot{y}_k \\ \ddot{y}_l \end{bmatrix} = \begin{bmatrix} x_3 \\ x_4 \\ \frac{m_l g (x_2 - x_1)}{m_k l_s \sqrt{1 - \frac{(x_2 - x_1)^2}{l_s^2}}} \\ -\frac{g (x_2 - x_1)}{l_s \sqrt{1 - \frac{(x_2 - x_1)^2}{l_s^2}}} \end{bmatrix} + \underbrace{\begin{bmatrix} 0 \\ 0 \\ \frac{F_k}{m_k} \\ 0 \end{bmatrix}}_{\underline{G} u}. \quad (5)$$

3. CONTROL DESIGN BASED ON THE PORT-HAMILTONIAN STRUCTURE

The derived state space representation shall be stated as Port-Hamiltonian system for control design, see (Lozano et al. [2000], van der Schaft [2000]). Starting from the PH-structure, first a passivity-based controller is designed using the energy-shifting method. Here, the total energy of the system is assigned a minimum in the desired crane load position that is to be stabilized. In extension to this controller, also the interconnection as well as the system damping can be changed by employing the IDA-PBC-approach, c.f. Rodriguez et al. [2000].

3.1 PH-description of the y -axis

In the following the system description in Port-Hamiltonian form shall be established. The total energy H of the crane axis to be controlled consists of the sum of kinetic and potential energy, i.e. $H = T + V$. This total energy function H has to be partially differentiated w.r.t. the state variables \underline{x} . This results in the column vector

$$\nabla_{\underline{x}} H = \begin{bmatrix} -\frac{m_l g (x_2 - x_1)}{l_s \sqrt{1 - \frac{(x_2 - x_1)^2}{l_s^2}}} \\ \frac{m_l g (x_2 - x_1)}{l_s \sqrt{1 - \frac{(x_2 - x_1)^2}{l_s^2}}} \\ m_k x_3 \\ m_l x_4 \end{bmatrix}. \quad (6)$$

Now the interconnection matrix \underline{J} and the damping matrix \underline{R} need to be determined such that they comply with $\underline{J} = -\underline{J}^T$ und $\underline{R} = \underline{R}^T$. The PH-system description has the form

$$\dot{\underline{x}} = (\underline{J} - \underline{R}) \nabla_{\underline{x}} H + \underline{G} u. \quad (7)$$

By comparison of (5) and (6), the interconnection matrix \underline{J} and the damping matrix \underline{R}

$$\underline{J} = \begin{bmatrix} 0 & 0 & \frac{1}{m_k} & 0 \\ 0 & 0 & 0 & \frac{1}{m_l} \\ -\frac{1}{m_k} & 0 & 0 & 0 \\ 0 & -\frac{1}{m_l} & 0 & 0 \end{bmatrix}, \quad \underline{R} = \begin{bmatrix} 0 & 0 & 0 & 0 \\ 0 & 0 & 0 & 0 \\ 0 & 0 & 0 & 0 \\ 0 & 0 & 0 & 0 \end{bmatrix} \quad (8)$$

can be determined. Based on this system representation the control law can be derived following either the energy-shifting-method or the IDA-PBC-approach.

3.2 Energy-shifting for the y-axis

This design approach aims at shaping the total energy of the closed-loop by choosing a appropriate energy function H_d such that the system is stabilized at the desired crane load position. The desired energy function $H_d = H + H_a$, which is given as the sum of the open-loop energy function H and an additional energy term H_a , can be determined as solution of the following partial differential equation

$$(\underline{J} - \underline{R}) \nabla_{\underline{x}} H + \underline{G} u = (\underline{J} - \underline{R}) \nabla_{\underline{x}} H_d. \quad (9)$$

Re-arranging and solving for the input term leads to

$$\underline{G} u = (\underline{J} - \underline{R}) \nabla_{\underline{x}} H_a. \quad (10)$$

A componentwise consideration results in four equations: three equations involving partial derivatives for the calculation of the additional energy function H_a and another equation that determines the control law u

$$0 = \frac{1}{m_k} \frac{\partial H_a}{\partial x_3}, \quad 0 = \frac{1}{m_l} \frac{\partial H_a}{\partial x_4}, \quad (11)$$

$$\underbrace{F_k}_{=u} = -\frac{\partial H_a}{\partial x_1}, \quad 0 = -\frac{1}{m_l} \frac{\partial H_a}{\partial x_2}.$$

It becomes obvious that the energy function to be determined H_a is independent of the state variables x_2 , x_3 and x_4 . As a result, it is only a function of the state variable $x_1 = y_k$, i. e. $H_a = f(x_1)$. In order to achieve stability of the closed-loop system, the following necessary and sufficient conditions must be fulfilled at the desired equilibrium state vector \underline{x}^* : the total energy function of

the closed-loop $H_d = H + H_a$ must have a minimum at \underline{x}^* . This can be investigated by means of the gradient vector $\nabla_{\underline{x}} H_d$ and the Hessian $\nabla_{\underline{x}}^2 H_d$.

$$\nabla_{\underline{x}} H_d \Big|_{\underline{x}=\underline{x}^*} = \begin{pmatrix} \frac{\partial H_a}{\partial x_1} - \frac{m_l g (x_2 - x_1)}{l_s \sqrt{1 - \frac{(x_2 - x_1)^2}{l_s^2}}} \\ \frac{m_l g (x_2 - x_1)}{l_s \sqrt{1 - \frac{(x_2 - x_1)^2}{l_s^2}}} \\ m_k x_3 \\ m_l x_4 \end{pmatrix} \Big|_{\underline{x}=\underline{x}^*}$$

$$= \begin{pmatrix} \frac{\partial H_a}{\partial x_1} \Big|_{\underline{x}=\underline{x}^*} \\ 0 \\ 0 \\ 0 \end{pmatrix} \stackrel{!}{=} \underline{0}. \quad (12)$$

An extremum is obtained if $\frac{\partial H_a}{\partial x_1} \Big|_{\underline{x}=\underline{x}^*} = 0$ holds. A minimum of the closed-loop system in the desired equilibrium state \underline{x}^* exists if the Hessian is positive definite at this point

$$\nabla_{\underline{x}}^2 H_d \Big|_{\underline{x}=\underline{x}^*} = \begin{pmatrix} \gamma + \frac{\partial^2 H_a}{\partial x_1^2} & -\gamma & 0 & 0 \\ -\gamma & \gamma & 0 & 0 \\ 0 & 0 & m_k & 0 \\ 0 & 0 & 0 & m_l \end{pmatrix} \Big|_{\underline{x}=\underline{x}^*}$$

$$= \begin{pmatrix} \frac{m_l g}{l_s} + \frac{\partial^2 H_a}{\partial x_1^2} \Big|_{\underline{x}=\underline{x}^*} & -\frac{m_l g}{l_s} & 0 & 0 \\ -\frac{m_l g}{l_s} & \frac{m_l g}{l_s} & 0 & 0 \\ 0 & 0 & m_k & 0 \\ 0 & 0 & 0 & m_l \end{pmatrix} \stackrel{!}{>} 0,$$

$$\text{with } \gamma = \frac{m_l g}{l_s \left(1 - \frac{(x_2 - x_1)^2}{l_s^2}\right)^{3/2}}. \quad (13)$$

A reasonable choice of the energy function is

$$H_a(x_1) = \frac{K}{2} (x_1 - x_{1,d})^2. \quad (14)$$

The proportional controller gain K is chosen positive, i.e. $K > 0$, to guarantee a positive definite Hessian. The variable $x_{1,d}$ denotes the desired trolley position that must be identical to the desired crane load position, considering a vanishing steady-state rope angle φ_y . The energy-shifting control approach results in a proportional control law

$$u = F_k = -\frac{\partial H_a}{\partial x_1} = -K (x_1 - x_{1,d}). \quad (15)$$

However, the energy-shifting does not affect the damping properties of the given crane axis as opposed to the IDA-PBC-approach employed in the following.

3.3 Control design based on the IDA-PBC-method

In order to improve the closed-loop dynamics, the damping properties shall be modified by using IDA-PBC. Here, not only the energy function H_d of the closed-loop system is specified but also damping is injected by modifying the given damping matrix R by an additional matrix R_a . Moreover, the given interconnection matrix J is extended by an additional matrix J_a . Thereby, two new matrices are introduced in the system description, which lead to the resulting matrices $J_d = J + J_a$ und $R_d = R + R_a$. This results in the following Port-Hamiltonian system description

$$\begin{aligned} (\underline{J} - \underline{R}) \nabla_{\underline{x}} H + \underline{G} u &= (\underline{J}_d - \underline{R}_d) \nabla_{\underline{x}} H_d, \\ \Leftrightarrow (\underline{J} - \underline{R}) \nabla_{\underline{x}} H + \underline{G} u &= [(\underline{J} - \underline{R}) + (\underline{J}_a - \underline{R}_a)] \cdot \\ &\quad \cdot [\nabla_{\underline{x}} H + \nabla_{\underline{x}} H_a]. \end{aligned} \quad (16)$$

This partial differential equation can be solved for the input term

$$\underline{G} u = (\underline{J}_a - \underline{R}_a) \nabla_{\underline{x}} H + (\underline{J}_d - \underline{R}_d) \nabla_{\underline{x}} H_a. \quad (17)$$

The additional interconnection matrix \underline{J}_a and damping matrix \underline{R}_a have been chosen as follows:

$$J_a = \begin{bmatrix} 0 & 0 & j_{13} & 0 \\ 0 & 0 & 0 & j_{24} \\ -j_{13} & 0 & 0 & 0 \\ 0 & -j_{24} & 0 & 0 \end{bmatrix}, \quad R_a = \begin{bmatrix} 0 & 0 & 0 & 0 \\ 0 & 0 & 0 & 0 \\ 0 & 0 & R & 0 \\ 0 & 0 & 0 & 0 \end{bmatrix}, \quad (18)$$

with $j_{13} = -m_k^{-1} + \alpha$ and $j_{24} = -m_l^{-1} + \alpha$. The energy function H_a and the corresponding stabilizing feedback control law are obtained as the solution of the following partial differential equations, where the third equation determines the control law

$$\begin{aligned} 0 &= \alpha \left(\frac{\partial H_a}{\partial x_3} + m_k x_3 \right) - x_3, \quad 0 = \alpha \frac{\partial H_a}{\partial x_4} - x_4, \\ \frac{u}{m_k} &= R \frac{\partial H_a}{\partial x_3} - \alpha \frac{\partial H_a}{\partial x_1} - \frac{m_l g (x_2 - x_1)}{m_k \sqrt{l_s^2 - (x_2 - x_1)^2}}, \\ 0 &= \frac{g (x_2 - x_1)}{\sqrt{l_s^2 - (x_2 - x_1)^2}} - \alpha \frac{\partial H_a}{\partial x_2}. \end{aligned} \quad (19)$$

The solution of (19) is given by the additive energy function

$$\begin{aligned} H_a &= \frac{g (x_2 - x_1)^2}{\alpha \sqrt{l_s^2 - (x_2 - x_1)^2}} - \frac{g l_s^2}{\alpha \sqrt{l_s^2 - (x_2 - x_1)^2}} \\ &\quad + \frac{x_3^2 + x_4^2 - \alpha m_k x_3^2}{\alpha} + \Gamma, \end{aligned} \quad (20)$$

with $\Gamma = f(x_1)$. It can be easily shown that the following choice of the arbitrary function

$$\Gamma = \frac{K}{2} (x_1 - x_{1,d})^2 \quad (21)$$

for all proportional gains $K > 0$ and couplings $\alpha > 0$ leads to a closed-loop energy function H_d with a

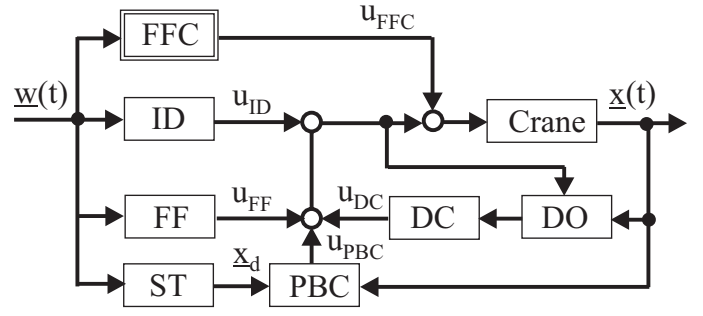


Fig. 3. Control implementation

global minimum in the desired crane load position $\underline{x}^* = (x_{1,d} \ x_{2,d} \ 0 \ 0)^T = (x_{1,d} \ x_{1,d} \ 0 \ 0)^T$. With the known energy function the IDA-PB control law u can be calculated from the third equation of (19)

$$\begin{aligned} u &= u_{PBC} = R m_k x_3 \left(\frac{1}{\alpha} - m_k \right) - K \alpha m_k (x_1 - x_{1,d}) \\ &\quad + \frac{g (m_l x_1 - m_k x_1 + m_k x_2 - m_l x_2)}{\sqrt{l_s^2 - (x_2 - x_1)^2}}. \end{aligned} \quad (22)$$

4. IMPLEMENTATION OF THE CRANE CONTROL

In addition to the passivity-based control u_{PBC} , some structural extension have turned out to be useful at implementation to improve trajectory tracking (Fig. 3). Hence, the stabilizing PBC is extended with feedforward control action based on an inverse system model. This feedforward control involves the following parts:

- (1) inverse dynamics control action u_{ID} based on the equation of motion without disturbance forces
- (2) feedforward compensation u_{FFC} of nonlinear friction and damping forces as main disturbances
- (3) a feedforward control action u_{FF} corresponding to the feedback control part u_{PBC}

The latter part u_{FF} is necessary to compensate for the feedback control in the ideal case if the design model matches the real system exactly. Then, the first two feedforward parts $u_{ID} + u_{FFC}$ would lead to a perfect trajectory tracking. In the given case of an imperfect system model with remaining uncertainties and disturbances, feedback control is mandatory and only a certain part is compensated by $u_{ID} + u_{FFC}$. A trajectory planning module yields the desired values

$$\underline{w} = [y_{l,d}, \dot{y}_{l,d}, \ddot{y}_{l,d}, \ddot{y}_{l,d}]^T \quad (23)$$

for the crane load position $y_{l,d}$, as well as its first three time derivatives. For the feedforward control, however, the corresponding desired values for the trolley position $y_{k,d}$ and its time derivative $\dot{y}_{k,d}$ are required. As the system under consideration is differentially flat with the crane load position as flat control output, all the desired state variables and the control input can be calculated. In the implementation, the following linearized relationships have been used in the state transformation ST

$$y_{k,d} = y_{l,d} + \frac{l_s}{g} \ddot{y}_{l,d}, \quad \dot{y}_{k,d} = \dot{y}_{l,d} + \frac{l_s}{g} \ddot{y}_{l,d}. \quad (24)$$

With the control structure described above, sufficiently small control errors could be achieved. Nevertheless, the

implemented model-based friction compensation can be significantly improved by an additional reduced-order disturbance observer DO as well as an disturbance compensation DC as described in Aschemann et al. [2000]. The complete control structure is adapted to the varying system parameters load mass m_l and rope length l_s by gain-scheduling.

4.1 Control of the x -axis

The designed passivity-based control for the y -axis shall be used for the x -axis control as well. The crane bridge, however, is equipped with two electric drives, which have to be properly actuated to achieve both the desired motion in x -direction but also a vanishing position difference of both bridge sides. Due to an excentric trolley position on the bridge and different friction forces acting on the corresponding drives, an active synchronization of both bridge drives have to be provided instead of a simple division of the according passivity-based control action u_{PBC} in the form $u_{b,l} = u_{b,r} = 0.5 \cdot u_{PBC}$. The active synchronization is achieved by an underlying PD-control loop of high bandwidth, i.e. $m_\varphi = -K_{p,GLR} \varphi_{xb} - K_{d,GLR} \dot{\varphi}_{xb}$. The required force distribution can be derived from the following system of equations

$$\begin{aligned} \begin{bmatrix} u_{PBC} \\ m_\varphi \end{bmatrix} &= \begin{bmatrix} 1 & 1 \\ -\frac{l_{br}}{2} & \frac{l_{br}}{2} \end{bmatrix} \begin{bmatrix} u_{b,r} \\ u_{b,l} \end{bmatrix}, \\ \Leftrightarrow \begin{bmatrix} u_{b,r} \\ u_{b,l} \end{bmatrix} &= \begin{bmatrix} \frac{1}{2} & -\frac{1}{l_{br}} \\ \frac{1}{2} & \frac{1}{l_{br}} \end{bmatrix} \begin{bmatrix} u_{PBC} \\ m_\varphi \end{bmatrix}. \end{aligned} \quad (25)$$

Thereby, the control design for the y -axis can be used for the bridge position control as well. The x -position of the trolley depends on the y -position on the bridge and on the two position coordinates of the bridge, i.e. $x_{b,r}$ und $x_{b,l}$. This position can be calculated as follows:

$$x_k = x_{b,r} + (x_{b,l} - x_{b,r}) \left(\frac{1}{2} + \frac{y_k}{l_{br}} \right). \quad (26)$$

Consequently, with the bridge mass m_b the outer control loop provides the resulting drive force u_{PBC} in x -direction.

$$\begin{aligned} u_{PBC} &= R m_b \dot{x}_k \left(\frac{1}{\alpha} - m_b \right) - K \alpha m_b (x_k - x_{k,d}) \\ &+ \frac{g (m_l x_k - m_b x_k + m_b x_l - m_l x_l)}{\sqrt{l_s^2 - (x_l - x_k)^2}}. \end{aligned} \quad (27)$$

5. EXPERIMENTAL RESULTS

Tracking performance as well as steady-state accuracy w.r.t. the crane load position have been investigated by experiments with a 5 t -overhead travelling crane. First, the focus has been on the tracking behaviour of the y -axis with a constant rope length of $l_s = 4$ m . The results are shown in terms of the rope angle in fig. 4. Second, a sequence of diagonal movements of the crane load has been specified in the xy -plane with constant rope length $l_R = 5$ m . The resulting tracking errors are depicted in fig. 5. Third, the tracking of desired trajectories in the xyz -workspace involving variations in the rope length has been investigated, see fig. 6.

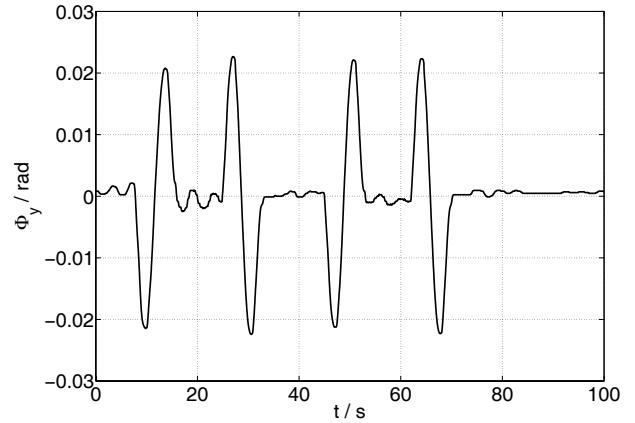


Fig. 4. Damping of load oscillations with constant rope length $l_R = 4$ m

6. CONCLUSIONS

This paper presents a gain-scheduled passivity-based control design for the translational axes of a 5 t -overhead travelling crane. The feedback control is extended by feedforward control exploiting the differential flatness of the system. Furthermore, a reduced-order disturbance observer takes into account the remaining model uncertainties stemming from nonlinear friction acting on the trolley. The efficiency of the proposed control is shown by experimental results involving tracking of desired trajectories within the three-dimensional workspace. Maximum tracking errors are approx. 2 cm .

REFERENCES

- H. Aschemann, S. Lahres, O. Sawodny, and E.P. Hofer. *Gain Scheduled Motion Control of an Overhead Travelling Crane*. IFAC Conference on Control System Design, Bratislava, pages 599–604, 2000.
- H. Aschemann. *Optimale Trajektorienplanung sowie modellgestützte Steuerung und Regelung für einen Brückenkran (in German)*. Fortschrittberichte VDI, Reihe 8, Nr. 929, VDI-Verlag, Düsseldorf, 2002.
- F. Boustany, B. d'Andrea-Novel. *Adaptive Control of an Overhead Crane Using Dynamic Feedback Linearization and Estimation Design*. IEEE International Conference on Robotics and Automation, Nice, France, pages 1963–1968, 1992.
- A. Janzen. *Passivitätsbasierte Regelung mechatronischer Systeme (in German)*. Diploma thesis, University of Ulm, Germany, 2006.
- R. Lozano, B. Brogliato, O. Egeland, and B. Maschke. *Dissipative Systems Analysis and Control: Theory and Applications*. Springer, 2000.
- H.T. Nguyen. *State Variable Feedback Controller for an Overhead Crane*. *Journal of Electrical and Electronics Engineering*, 14:75–84, 1994.
- H. Rodriguez, R. Ortega, and I. Mareels. *A Novel Passivity-Based Controller for an Active Magnetic Bearing Benchmark Experiment*. Proc. of the ACC 2000, Chicago, Illinois, 2000.
- A. van der Schaft. *L₂-Gain and Passivity Techniques in Nonlinear Control*. Springer, 2000.

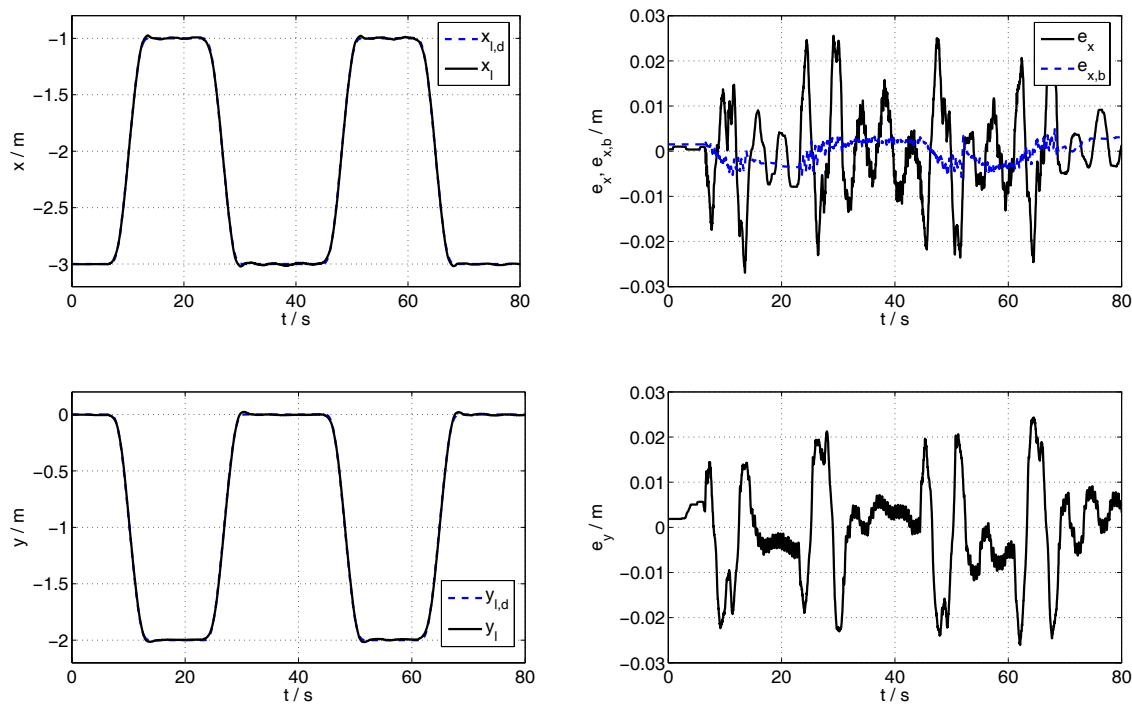


Fig. 5. Synchronised movement in the xy -plane with constant rope length $l_R = 5\text{ m}$

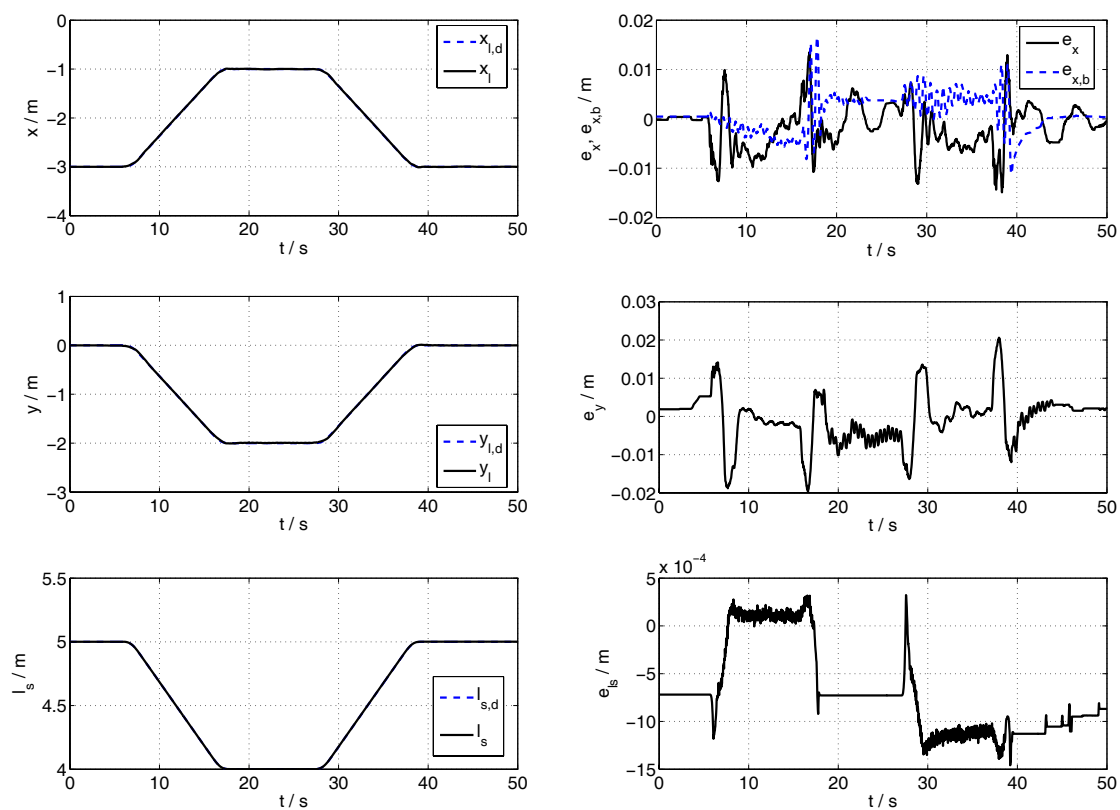


Fig. 6. Synchronised movement in the xyz -workspace with varying rope length